washed with hot benzene (2 × 20 mL) and dried in vacuo. The colorless crystals of *phosphonium salt* **17** so obtained (14.81 g, 110%) contained benzene by ^{1}H NMR which could not be removed by heating of the sample in vacuo. The salt was used without further purification in the next reaction.

17: mp 85.5–88.5 °C; IR ($CHCl_3$) 2940 (s), 1440 (s), 1240 (s), 1115 (s), 995 (m), 715 (s), 685 (s), 655 (s) cm^{-1}; ^{1}H NMR (250 MHz, $CDCl_3$) δ 1.36–1.38 (m, 2 H), 1.48–1.57 (m, 2 H), 2.17 (br s, 2 H), 2.48–2.53 (m, 2 H), 4.85 (dd, J = 7.7, 15.3 Hz, 2 H), 5.42 (m, 1 H, 6.96–7.23 (comp m, 4 H), 7.66–7.98 (comp m, 15 H); chemical ionization mass spectrum, m/e 433.2015 (M − Br calcd for $C_{31}H_{30}P$, 433.2085).

(***E*,*E***)-**Bis(benzosuberanylidenyl)ethane** (**3**). *n*-Butyllithium (1.46 mL, 2.40 M in hexanes, 3.50 mmol) was added to a suspension of phosphonium salt **17** (2.00 g, 3.90 mmol) in 20 mL of benzene/THF (1:1) at 0 °C under argon until a faint yellow color persisted, and a further 1.46 mL (3.50 mmol) was added. The suspension was stirred at room temperature for 45 min, after which 1-benzosuberone (0.56 g, 3.5 mmol) was added. The reaction mixture was heated to reflux for 22 h, then allowed to cool, poured into water, and extracted with ether. Combined organic extracts were washed with brine, dried over magnesium sulfate, and concentrated in vacuo. Flash column chromatography (hexanes:$CHCl_3$, 1:1) followed by crystallization from methylene chloride/hexanes gave the *diene* (**3**) as colorless prisms (144 mg, 13%): mp 186.5–187.5 °C; IR ($CHCl_3$) 3065 (w), 3010 (m), 2935 (s), 2855 (m), 1705 (w), 1600 (w), 1480 (m), 1450 (m), 890 (w) cm^{-1}; ^{1}H NMR (250 MHz, $CDCl_3$) δ 1.74–1.76 (m, 8H) 2.58 (br s, 4 H), 2.76–2.78 (m, 4 H), 6.43 (s, 2 H), 7.09–7.28 (comp m, 8 H); ^{13}C NMR (69.5 MHz, $CDCl_3$) δ 27.0, 27.6, 29.6, 34.8, 123.5, 126.2, 126.9, 127.6, 128.8, 139.9, 144.6, 145.2; λ_{max} (hexanes) 292.4 and 202.0 nm (ε 27 000 and 25 000); chemical ionization mass spectrum, m/e 315.2110 (M + H calcd for $C_{24}H_{27}$, 315.2113). Anal. Calcd for $C_{24}H_{26}$: C, 91.67; H, 8.33. Found: C, 91.48; H, 8.20.

Acknowledgment. This research was supported by the National Science Foundation—Laboratory for Research on the Structure of Matter (LRSM), Grant No. DMR-85-19059, and in part by grants to R.M.H. and A.B.S. from NSF and NIH. In addition, we thank Drs. G. Furst, J. Dykins, and P. Carroll, Directors of the University of Pennsylvania Spectroscopic Facilities, for aid in obtaining respectively the high-field NMR, high-resolution mass spectral, and X-ray crystallographic data and Wing Sau Young for determining the UV spectral data.

Core and Valence-Shell Electronic Excitation of Nickel Tetracarbonyl by High-Resolution Electron Energy Loss Spectroscopy

Glyn Cooper, Kong Hung Sze, and C. E. Brion*

Contribution from the Department of Chemistry, University of British Columbia, Vancouver, B.C., Canada V6T 1Y6. *Received September 30, 1988*

Abstract: Core (inner-shell) and valence-shell electron energy loss spectra of $Ni(CO)_4$ are compared with corresponding spectra of free CO under kinematic conditions where the spectra are dominated by dipole-allowed transitions. The inner-shell spectra encompass the C 1s, O 1s, and Ni 3p excitation and ionization regions of $Ni(CO)_4$. The C and O 1s spectra of $Ni(CO)_4$ show some major similarities to those of free CO. In particular both the C 1s and the O 1s inner-shell spectra of both molecules exhibit intense 1s → π* and 1s → σ* transitions. For the case of the C 1s → π* transitions vibrational structure is resolved for both $Ni(CO)_4$ and CO. There are also significant differences, however, which are related to the different manifolds of final states available in the two molecules. Tentative assignments are suggested for the $Ni(CO)_4$ spectra using molecular orbital energy level and term value considerations. The implications of the results for studying dπ → pπ back-bonding in transition-metal carbonyl complexes are discussed.

Transition-metal carbonyl complexes have been the subject of a large amount of spectroscopic measurement[1-15] and theoretical investigation[2,7,13,16-26] due to their high photochemical and catalytic activity.[27-32] They have been used as prototype models for the bonding of CO to transition-metal surfaces[10,33-35] and serve as model systems for many organometallic complexes. An understanding of the electronic structures of transition-metal carbonyl complexes is thus of great importance to diverse areas of practical importance.

Although $Ni(CO)_4$ is the simplest example of the tetrahedral metal carbonyl species, its valence-shell photoabsorption spectrum has received little attention, and to date no core excitation spectra

(1) Reutt, J. E.; Wang, L. S.; Lee, Y. T.; Shirley, D. A. *Chem. Phys. Lett.* **1986**, *126*, 399.
(2) Hillier, I. H.; Guest, M. F.; Higginson, B. R.; Lloyd, D. R. *Mol. Phys.* **1974**, *27*, 215.
(3) Chen, H. W.; Jolly, W. L. *Inorg. Chem.* **1979**, *18*, 2548.
(4) Chambers, S. A. Ph.D. Thesis, Oregon State University, 1978.
(5) Bancroft, G. M.; Boyd, B. D.; Creber, D. K. *Inorg. Chem.* **1978**, *17*, 1008.
(6) Lever, A. B. P.; Ozin, G. A.; Hanlan, A. J. L.; Power, W. J.; Gray, H. B. *Inorg. Chem.* **1979**, *18*, 2088.
(7) Schreiner, A. F.; Brown, T. L. *J. Am. Chem. Soc.* **1968**, *90*, 3366.
(8) Koerting, C. F.; Walzl, K. N.; Kupperman, A. *J. Chem. Phys.* **1987**, *86*, 6646.
(9) Cooper, G.; Green, J. C.; Payne, M. P.; Dobson, B. R.; Hillier, I. H. *J. Am. Chem. Soc.* **1987**, *109*, 3836.
(10) Plummer, E. W.; Salaneck, W. R.; Miller, J. S. *Phys. Rev. B* **1978**, *18*, 1673.
(11) Loubriel, G.; Plummer, E. W. *Chem. Phys. Lett.* **1979**, *64*, 234.
(12) Chastain, S. K.; Mason, R. W. *Inorg. Chem.* **1981**, *20*, 1395.
(13) Beach, N. A.; Gray, H. B. *J. Am. Chem. Soc.* **1968**, *90*, 5713.
(14) Iverson, A.; Russell, B. R. *Chem. Phys. Lett.* **1970**, *6*, 307.
(15) Tossell, J. A.; Moore, J. H.; Olthoff, K. *J. Am. Chem. Soc.* **1984**, *106*, 823.
(16) Hillier, I. H.; Saunders, V. R. *Mol. Phys.* **1971**, *22*, 1025.
(17) Loubriel, G. *Phys. Rev. B* **1979**, *20*, 5339.
(18) Rosch, N.; Jorg, H.; Kotzian, M. *J. Chem. Phys.* **1987**, *86*, 4038.
(19) Baerends, E. J.; Ros, P. *Mol. Phys.* **1975**, *30*, 1735.
(20) Ford, P. C.; Hillier, I. H. *J. Chem. Phys.* **1983**, *80*, 5664.
(21) Yang, C. Y.; Arratia-Perez, R.; Lopez, J. P. *Chem. Phys. Lett.* **1984**, *107*, 112.
(22) Dick, B.; Freund, H.-J.; Hohlneicher, G. *Mol. Phys.* **1982**, *45*, 427.
(23) Johnson, J. B.; Klemperer, W. G. *J. Am. Chem. Soc.* **1977**, *99*, 7132.
(24) Sherwood, D. E.; Hall, M. B. *Inorg. Chem.* **1980**, *19*, 1905.
(25) Bursten, B. E.; Freier, B. G.; Fenske, R. F. *Inorg. Chem.* **1980**, *19*, 1810.
(26) Bauschlicher, Jr., C. W.; Bagus, P. S. *J. Chem. Phys.* **1984**, *81*, 5889.
(27) Wrighton, M.; Hammond, G. S.; Gray, H. B. *J. Organomet. Chem.* **1974**, *70*, 283.
(28) Koerner van Gustorf, E.; Guerals, F. W. *Fortsch. Chem. Forsch.* **1969**, *13*, 366.
(29) Lewandos, G. S.; Pettit, R. *J. Am. Chem. Soc.* **1971**, *93*, 7087.
(30) Leigh, G. L.; Fischer, E. O. *J. Organomet. Chem.* **1965**, *4*, 461.
(31) Fischer, E. O.; Fritz, H. P. *Angew. Chem.* **1961**, *73*, 353.
(32) Wrighton, M. *Chem. Rev.* **1974**, *74*, 401, and references therein.
(33) Muetterties, E. *Science* **1976**, *194*, 1150.
(34) Muetterties, E. *Science* **1977**, *196*, 839.
(35) Fruend, H.-J.; Plummer, E. W. *Phys. Rev. B* **1981**, *23*, 4859.

0002-7863/89/1511-5051$01.50/0

have been reported. Previous photoabsorption studies of $Ni(CO)_4$[6,7] have been limited to excitation energies below the quartz cutoff frequency (~7 eV), and even within this limited region the spectrum is not well understood. Valence-shell[1,2] and core-level[3,4] photoelectron spectra of $Ni(CO)_4$ and the corresponding ionization energies have, however, been reported.

Inner-shell electron energy loss spectroscopy (ISEELS) at small momentum transfer is a viable alternative[36-38] to the use of synchrotron radiation for photoabsorption studies in the soft X-ray region of the spectrum (i.e., 200–1000-eV equivalent photon energy). ISEELS is particularly advantageous in the region of carbon, nitrogen, and oxygen 1s (K shell) excitation (≃300, 400, and 550 eV, respectively) where approximately an order of magnitude better energy resolution is available[36-39] than in existing soft X-ray photoabsorption spectrometers. In ISEELS it is therefore possible to obtain vibrational resolution in C 1s[39-42] and N 1s[38,39,43] molecular core spectra. For O 1s and more deeply bound levels the core hole lifetime is already too short to support molecular vibration.[39] In addition photoabsorption in the C 1s region is complicated by diffraction grating and mirror contamination due to surface-adsorbed films of carbon-containing material. Similarly oxygen-containing materials in the grating can also cause spectral complications.

Unlike the valence-shell electronic excitation spectrum, the C 1s and O 1s inner-shell spectra of carbon monoxide exhibit very strong resonantly enhanced features, namely, the dominant 1s → π^* resonances below the respective 1s edges, and the 1s → σ^* resonances which lie in the continuum.[39,41,42,44] In contrast the 1s → Rydberg transitions make only a relatively small contribution to the spectrum. The resonant enhancement is caused by interaction of the outgoing core electron with the anisotropic molecular field in selected inner-shell excitation channels. This interaction results in strong local concentrations of oscillator strength. Quantitative theoretical interpretations of these core spectra include the MO treatment of Rescigno et al.[45] and the MS-Xα multiple scattering calculations of Dehmer and Dill.[46] In the MO picture core electrons are excited to the empty π^*, σ^*, and Rydberg levels, while in the MS-Xα approach the resonant enhancements appear as phase shifts in the $l = 2$ (π^*) and $l = 3$ (σ^*) outgoing partial waves and are often referred to as d-wave and f-wave resonances, respectively. Such strong core excitation resonances are a commonly observed feature of inner-shell excitation and photoabsorption spectra in a wide variety of molecules.[47] In addition to these interesting features, inner-shell spectra are potentially useful because they are easier to interpret than their valence-shell counterparts due to the unambiguous assignment of the initial (core) orbital. This is in marked contrast to the typical valence-shell situation where unequivocal assignment of the transitions is often complicated by the many closely spaced occupied valence orbitals.

With the above considerations in mind it is of interest to investigate the applicability of ISEELS methods to a study of transition-metal complexes. In particular the metal–ligand ($d\pi \rightarrow p\pi$) back-donation envisaged in models of the bonding in transition-metal carbonyl complexes involves receptor orbitals that correspond to the π^* orbitals of free CO. If localized π^* and σ^* resonances of the type observed in CO also occur in metal carbonyls, then a study of the energies and intensities of these spectral features should provide a sensitive probe of the metal–ligand bonding. Also the high-energy resolution uniquely available in the ISEELS technique in the soft X-ray equivalent photon energy region should provide further information through analysis of the vibrational structure in the C 1s → π^* spectra of the metal carbonyls.

With the above aims of further elucidating the electronic structure of $Ni(CO)_4$ and its highly excited electronic states, we have utilized electron energy loss spectroscopy to obtain the first reported core level (C 1s, O 1s, and Ni 3p) electronic spectra of gaseous nickel tetracarbonyl at vibrational resolution under experimental conditions where electronic dipole transitions dominate the spectra.[36-38] The high-resolution valence-shell excitation spectrum is also obtained over an extended energy range.

Experimental Section

The electron energy loss spectra were obtained by using a high-resolution spectrometer, the design and operation of which have been described previously.[48,49] Therefore, only a brief description of our experimental method is given here. A monochromated beam of electrons is accelerated to a selected impact energy in the range 1.0–3.7 keV and is scattered off the gaseous sample in a collision chamber. The inelastically scattered electrons are sampled at a mean scattering angle of 0° and are energy analyzed by a retarding lens/hemispherical electrostatic analyzer combination, operated in the constant pass energy mode. Under these conditions of forward scattering and high impact energies (i.e., small momentum transfer) the energy loss spectra are dominated by electric dipole transitions.[36-38] Energy resolution is in the range 0.03–0.31 eV fwhm. The valence-shell spectrum was calibrated by using the He 1s → 2p transition (21.218 eV), while the inner-shell spectra were put on an absolute energy scale by reference to the N 1s → π^* ($v = 1$) transition in N_2 (400.88 eV[50]). The small amount of free CO evident in the valence-shell spectrum of $Ni(CO)_4$ provided an additional check on peak positions.[39,51] In practice the calibration corrections were found to be very small (typically <0.05 eV) due to the efficient differential pumping of different regions of the spectrometer.[48,49]

The $Ni(CO)_4$ was obtained from a lecture bottle supplied by Matheson Chemicals Inc. The sample was purified by repeated freeze/thaw cycles of the lecture bottle by using an acetone/dry ice mixture and pumping off the residual gas (~5 times). By this means the amount of free CO in the $Ni(CO)_4$ cylinder could be reduced to an insignificant level. Valence-shell spectra were run before and after each inner-shell data collection period to verify that any contribution from free CO was negligible. Inner-shell and valence-shell spectra of free CO (Matheson Chemicals Inc.) were obtained under identical experimental conditions for comparison with the spectra of $Ni(CO)_4$ and to assist in the monitoring of CO impurity levels.

Results and Discussion

Electronic Structure of $Ni(CO)_4$. The electronic structure of $Ni(CO)_4$ has been the subject of many theoretical studies (for example, ref 2, 7, 16–19, 22, and 26). There is still not full agreement on the exact ordering of the valence energy levels, but the qualitative details of metal–ligand bonding are well understood. A qualitative MO diagram indicating the occupied and unoccupied orbitals of $Ni(CO)_4$ is given in Figure 1. The orbital ordering of the occupied valence levels is based on the calculation of ref 16.

In $Ni(CO)_4$ the Ni 3d orbitals are split by the tetrahedral ligand field into a higher energy triply degenerate ($9t_2$) and a lower energy doubly degenerate (2e) set of orbitals, while the CO 5σ and 1π orbitals are split into a manifold of levels with an energy spread ~4 eV[1,2] as illustrated in Figure 1. The CO 4σ orbitals are largely unaffected by complex formation and produce the very closely spaced $6t_2$ and $7a_1$ levels. The metal–ligand bonding is considered

(36) Brion, C. E.; Hamnett, A. H. *Adv. Chem. Phys.* **1981**, *45*, 1.
(37) Brion, C. E.; Daviel, S.; Sodhi, R.; Hitchcock, A. P. *AIP Conference Proceedings No. 94, X-Ray and Atomic Inner-shell Physics*; Crasemann, B., Ed.; American *Institute* of *Physics*: New York; 1982, p 429–446.
(38) Brion, C. E. *Comments At. Mol. Phys.* **1985**, *16*, 249.
(39) Hitchcock, A. P.; Brion, C. E. *J. Electron. Spectrosc. Relat. Phenom.* **1980**, *18*, 1.
(40) Hitchcock, A. P.; Brion, C. E. *J. Electron. Spectrosc. Relat. Phenom.* **1979**, *17*, 139.
(41) Tronc, M.; King, G. C.; Bradford, R. C.; Read, F. H. *J. Phys. B* **1976**, *9*, L555.
(42) Tronc, M.; King, G. C.; Read, F. H. *J. Phys. B* **1979**, *12*, 137.
(43) King, G. C.; Read, F. H.; Tronc, M. *Chem. Phys. Lett.* **1977**, *52*, 50.
(44) Wight, G. R.; Brion, C. E.; Van der Wiel, M. J. *J. Electron. Spectrosc. Relat. Phenom.* **1972**, *1*, 457.
(45) Rescigno, T. N.; Bender, C. F.; McKoy, B. V.; Langhoff, P. W. *J. Chem. Phys.* **1978**, *68*, 970, and references therein.
(46) Dill, D.; Dehmer, J. L. *J. Chem. Phys.* **1974**, *61*, 192.
(47) Hitchcock, A. P. *J. Electron. Spectrosc. Relat. Phenom.* **1982**, *25*, 245.
(48) Daviel, S.; Brion, C. E.; Hitchcock, A. P. *Rev. Sci. Instrum.* **1984**, *55*, 182.
(49) Sze, K. H.; Brion, C. E.; Tong, X. M.; Li, J. M. *Chem. Phys.* **1987**, *115*, 433.
(50) Sodhi, R. N. S.; Brion, C. E. *J. Electron. Spectrosc. Relat. Phenom.* **1984**, *34*, 363.
(51) Skerbele, A.; Dixon, M. A.; Lasettre, E. N. *J. Chem. Phys.* **1967**, *46*, 4161.

Table I. Experimental Energies, Term Values, and Possible Assignments of Features in the C 1s Electron Energy Loss Spectra of Nickel Tetracarbonyl and Carbon Monoxide[a]

$Ni(CO)_4$				CO			
feature	energy loss, eV	term value, eV	possible assgnt (final orbital)	feature	energy loss, eV	term value, eV	possible assgnt (final orbital)
1	287.6 (3)	6.17	π^* (v = 0)	1	287.40 (2)	8.70	$2\pi^*$ (v = 0)
	287.84 (3)	5.95	π^* (v = 1)		287.65 (1)	8.45	$2\pi^*$ (v = 1)
	288.08 (3)	5.72	π^* (v = 2)		287.89 (3)	8.21	$2\pi^*$ (v = 2)
2	289.34 (3)	4.44	Ni 4p, 4s				
3	290.21 (3)	3.57	CO $3s\sigma$; delocalized π^*	2	292.54 (5)	3.5	$3s\sigma$
				3	293.52 (5)	2.6	$3p\pi$
4	291.71 (12)	2.07	Ni 5p, 5s, Rydberg				
5	292.19 (12)	1.59	Rydberg	4	294.9 (1)	1.2	4s, 3d
6	293.75 (20)	0.03	Rydberg				
C 1s edge	293.78[b]			C 1s edge	296.1[c]		
7	296.2 (4)	−2.4	double excitation; l = 3 σ^*(Ni–C) shape resonance				
8	300.2 (4)	−6.5	double excitation; l = 3 σ^*(Ni–C) shape resonance	5	300.8 (1)	−4.7	double excitation
9	304.4 (4)	−10.7	l = 3 σ^*(C–O) shape resonance	6	304.0 (4)	−7.9	l = 3 σ^*(C–O) shape resonance

[a] From ref 39, calibrated by using ref 50. [b] From ref 3. [c] From ref 75.

Table II. Experimental Energies, Term Values, and Possible Assignments of Features in the O 1s Electron Energy Loss Spectra of Nickel Tetracarbonyl and Carbon Monoxide[a]

$Ni(CO)_4$				CO			
feature	energy loss, eV	term value, eV	possible assgnt (final orbital)	feature	energy loss, eV	term value, eV	possible assgnt (final orbital)
1	533.93 (12)	6.18	π^*	1	534.21 (9)	8.2	$2\pi^*$
2	536.51 (12)	3.6	CO $3s\sigma$; delocalized π^*	2	538.90 (8)	3.5	$3s\sigma$
				3	539.88 (8)	2.5	$3p\pi$
3	538.61 (12)	1.5	Rydberg	4	541.0 (1)	1.4	4s, 3d
O 1s edge	540.11[b]			O 1s edge	542.4[c]		
4	542.9 (4)	−2.8	l = 3 σ^*(Ni–C) shape resonance				
5	546.0 (4)	−5.9	l = 3 σ^*(Ni–C) shape resonance				
6	550.1 (4)	−10.0	l = 3 σ^*(C–O) shape resonance	5	551.0 (1)	−8.6	l = 3 σ^*(C–O) shape resonance

[a] From ref 39, calibrated by using ref 50. [b] From ref 3. [c] From ref 75.

to be generated through synergic CO → Ni σ-electron donation and Ni 3d → CO π back donation. The relative importance of the ligand → metal and metal → ligand interaction in bond formation has been the subject of considerable controversy.[2,7,16-19,22,26]

For ease of reference in the following discussion, the group of lowest energy unoccupied MOs (the $2t_1$, $10t_2$, and 3e) will be referred to as the $Ni(CO)_4$ π^* orbitals, since they are largely CO π^* in character. Similarly the manifold of levels derived from the CO 5σ and 1π orbitals (the 1e, $7t_2$, $8a_1$, $1t_1$, and $8t_2$) will be referred to as CO ($5\sigma + 1\pi$).

C 1s and O 1s Excitation Spectra. Figures 2 and 3 show C and O 1s excitation spectra of $Ni(CO)_4$, respectively, obtained with 3-keV incident electrons at a modest resolution of 0.305 eV fwhm. In each case the corresponding spectrum of free CO is also given on the same energy scale to facilitate comparisons between the spectra of the metal complex and the free ligand. The energies, term values and proposed assignments for the numbered features in these spectra are given in Tables I and II.

It is immediately obvious that the C and O 1s spectra of nickel tetracarbonyl show some obvious similarities with the respective corresponding spectra of free CO, and several of the features may be assigned by analogy. Clearly the counterparts of the below edge π^* and above edge σ^* resonances of CO[39,41,42,44] are present at quite similar corresponding energies and intensities in both the C 1s and O 1s $Ni(CO)_4$ ISEELS spectra (Figures 2 and 3). The overall degree of similarity is particularly striking for the O 1s spectra. There are also, however, some noteworthy differences in the region between the π^* and σ^* resonances particularly in the C 1s spectra. In contrast the O 1s spectra of $Ni(CO)_4$ and CO are much more similar in overall shape although as expected the Rydberg structure is less well resolved in the larger $Ni(CO)_4$ molecule. It is also noticeable that the relative contribution of Rydberg states is significantly less in the O 1s spectra of both $Ni(CO)_4$ and CO.

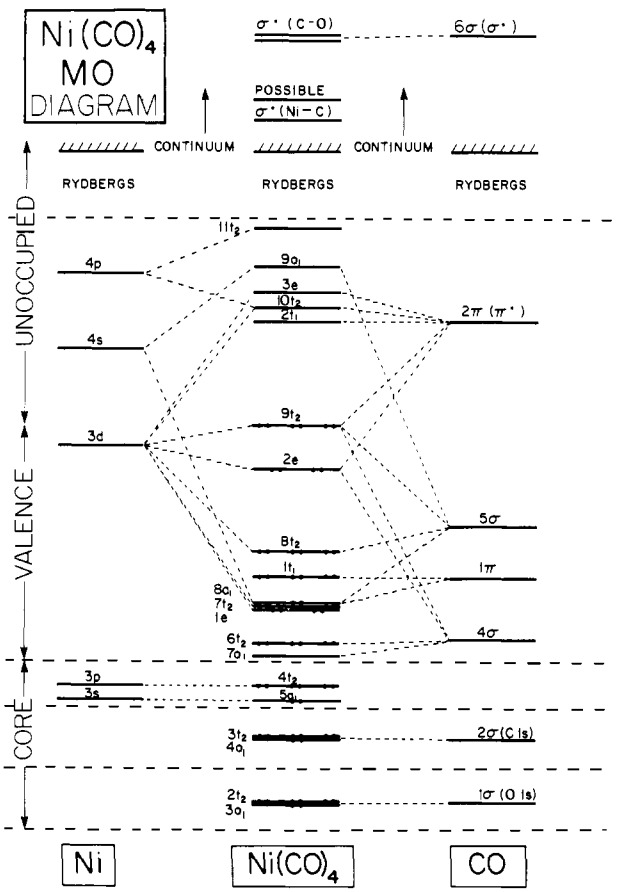

Figure 1. Qualitative molecular orbital energy level diagram for $Ni(CO)_4$.

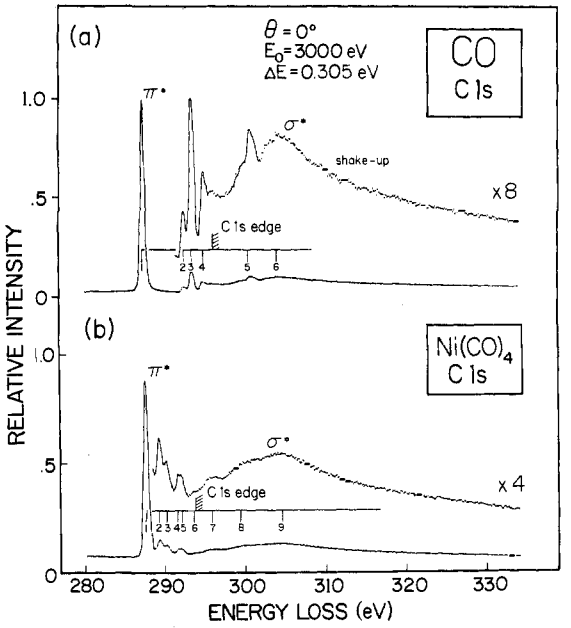

Figure 2. Carbon 1s electron energy loss spectra (fwhm = 0.305 eV) of (a) CO and (b) $Ni(CO)_4$.

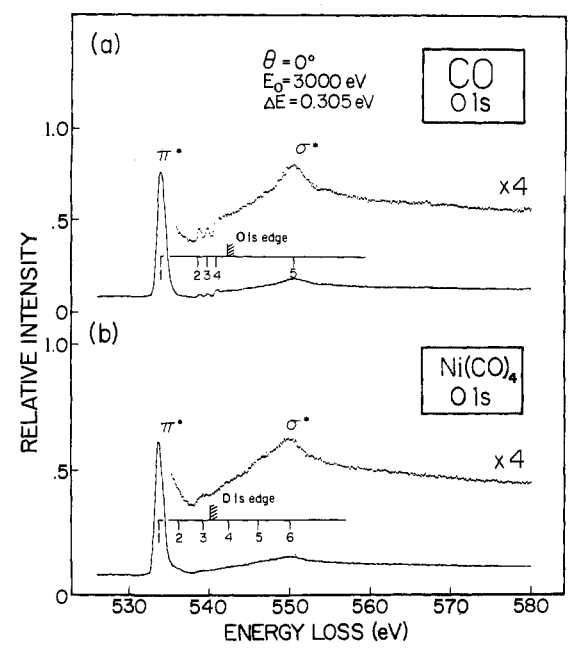

Figure 3. Oxygen 1s electron energy loss spectra (fwhm = 0.305 eV) of (a) CO and (b) $Ni(CO)_4$.

The most intense peaks in the $Ni(CO)_4$ spectra occur at approximately 6.2 eV below the respective C 1s and O 1s ionization thresholds[3,4] and may be confidently identified with 1s → π* (LUMO) transitions in $Ni(CO)_4$. It should be noted (Tables I and II) that the C 1s and O is ionization energies for the metal complex are both ~2.3 eV lower than for free CO. This has been shown to be due to greater orbital relaxation in $Ni(CO)_4$ accompanying ionization, rather than any significant differences in the 1s orbital energies.[35,52]

Figure 4b shows a high-resolution (0.068 eV) scan of the C 1s → π* peak in $Ni(CO)_4$. A spectrum of the corresponding transition in free CO at the same resolution is shown in Figure 4a for comparison. The latter spectrum exhibits vibrational structure consistent with earlier high-resolution ISEELS work.[39,41,42] The intensity distribution in the partially resolved structure in the

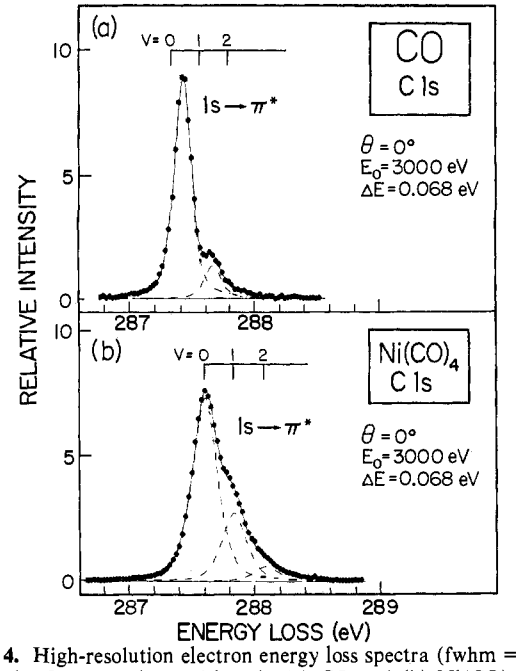

Figure 4. High-resolution electron energy loss spectra (fwhm = 0.068 eV) of the C 1s → π* transitions in (a) CO and (b) $Ni(CO)_4$. The dashed lined show fits of three Voigt profile curves to the experimental data (see text for details).

high-resolution spectrum of $Ni(CO)_4$ (Figure 4b) is not consistent with that expected on degeneracy grounds (≃3:3:2) for the three possible π* final electronic states ($2t_1$, $10t_2$, and 3e; see Figure 1). It is therefore more likely that these features are vibronic components of a single electronic transition. Also illustrated in Figure 4 are least-squares fits of three equal width Voigt profiles[53-55] (Gaussian/Lorentzian mix) to the experimental data. The parameters of these fits are as follows:

For CO: peak 1, position 287.40 eV,[50] fwhm 0.175 eV, relative area 1.0, Gaussian/Lorentzian area ratio 0.691; peak 2, position 287.65 eV, fwhm 0.175 eV, relative area 0.153, Gaussian/Lorentzian area ratio 0.691; peak 3, position 287.89 eV, fwhm 0.175 eV, relative area 0.015, Gaussian/Lorentzian area ratio 0.691.

For $Ni(CO)_4$: peak 1, position 287.61 eV, fwhm 0.232 eV, relative area 1.0, Gaussian/Lorentzian area ratio 0.889; peak 2, position 287.84 eV, fwhm 0.232 eV, relative area 0.370, Gaussian/Lorentzian area ratio 0.889; peak 3, position 288.08 eV, fwhm 0.232 eV, relative area 0.083, Gaussian/Lorentzian area ratio 0.889.

The best fits are obtained when the peaks have regular spacings of 0.245 ± 0.007 eV (1980 ± 55 cm^{-1}) for CO and 0.235 ± 0.007 eV (1900 ± 55 cm^{-1}) for $Ni(CO)_4$. The vibrational spacing for CO is in good agreement with previous work (2040 cm^{-1} [39]).

The fact that apparently only one (and not three) 1s → π* band is observed for $Ni(CO)_4$ can be understood in terms of the lowering in symmetry from tetrahedral in the ground state to C_{3v} in the 1s excited state, due to the localized nature of the C 1s (or O 1s) hole. SCF-LCAO-MO calculations for C 1s ionization in $Ni(CO)_4$[17,52] show that this leads to a doubly degenerate set of π* orbitals (e symmetry in C_{3v}) becoming localized on the CO group containing the core hole, while the remaining six π* orbitals are delocalized over the remaining ligands and have almost zero contribution from the C 1s ionized CO. The presence of a core hole also results in the localized π* orbitals having a substantially lower energy (~2.2 eV[52]) than the others. Similar considerations are expected to apply in the case of C 1s excitation, and also O 1s ionization and excitation. Thus, from considerations of spatial overlap, the probability of transitions to the localized π* orbitals

(52) Mitcheson, G. R.; Hillier, I. H. *J. Chem. Soc., Faraday Trans. 2* **1979**, *75*, 929.

(53) Olivero, J. J.; Longbothum, R. L. *J. Quantum Spectrosc. Radiat. Trans.* **1977**, *17*, 233.

(54) Voigt, W. *München Sitzker, Ak. Wiss. Math-Phys. Kl.* **1912**, *42*, 603.

(55) Kuhn, W. R.; London, J. *J. Atmos. Sci.* **1969**, *26*, 189.

will be much greater than for excitation into the other π^* MOs delocalized over the three neutral ligands, and transitions to the delocalized π^* orbitals would be expected to be located ~2 eV above the localized 1s → π^* band for both C 1s and O 1s excitation. By analogy with the situation in free CO it might therefore also be expected that resonant enhancement[39,41,42,44-46] of the C 1s → π^* transitions would also occur in the case of the *localized* π^* orbitals in $Ni(CO)_4$. This resonant enhancement in both $Ni(CO)_4$ and free CO is clearly present in the C 1s and O 1s spectra (Figures 2 and 3). This, together with the fact that the respective 1s → π^* and 1s → σ^* transition energies are almost identical for CO and $Ni(CO)_4$ in both the C 1s and O 1s spectra provides convincing evidence of the localized character of both the core hole and the occupied π^* and σ^* orbitals in C 1s and O 1s excited $Ni(CO)_4$. These observations are entirely consistent with the earlier theoretical predictions of the C 1s hole localization in core ionized $Ni(CO)_4$.[17,52,56]

The term values of the localized 1s → π^* bands in both the C 1s and the O 1s spectra are ~2.2 eV lower for nickel tetracarbonyl than for free CO gas (Tables I and II). Assuming that the C 1s orbital energies are almost equal in both compounds[35,52] would therefore imply a higher energy for the π^* final orbitals of $Ni(CO)_4$. Although of course the π^* orbitals involved in these transitions do not correspond directly with those in the neutral transition-metal complex, and we have the complicating factor of severe orbital relaxation, the decrease in term value nevertheless provides direct experimental evidence of how the energies of the CO 2π (π^*) orbitals are perturbed by their interaction with the Ni atom during complex formation. Further evidence is provided by the increase in C 1s → π^* transition energy of ~0.2 eV, although the O 1s → π^* energy is reduced by ~0.2 eV, presumably due to relaxation effects. Comparisons of term values and transition energies between a range of transition-metal carbonyl complexes should allow experimental determinations of the relative extent of $d\pi \rightarrow p\pi^*$ back bonding in these types of compounds. ISEELS studies of other carbonyl complexes are currently being carried out in this laboratory.[57]

The most striking difference between the vibrationally resolved C 1s → π^* band of $Ni(CO)_4$ and that of CO (Figure 4) is the relatively more intense excitation of the higher vibrational components $v = 1$ and $v = 2$ (v = vibrational quantum number) in the $Ni(CO)_4$ spectrum. This can be rationalized by realising that greater orbital relaxation accompanying C 1s excitation of the transition-metal complex (by analogy with the ionization process) will result in greater changes in molecular electron density distribution and hence larger changes in the C–O internuclear distance. The value of 0.235 eV (1900 cm^{-1}) obtained for the vibrational peak separation in $Ni(CO)_4$ is typical of a C=O stretching frequency, and the progression therefore can be confidently assigned to a C–O stretching mode. Since the core electron is being promoted into a π^* orbital localized on just one of the CO groups, vibrational excitation will be limited largely to this same ligand. The derived vibrational frequency (1900 cm^{-1}) can therefore be compared directly with the frequency of the C–O progression in the C 1s → π^* transition in free CO (1980 cm^{-1}) and with the vibrational modes of the ground state of $Ni(CO)_4$.

Because of the presence of several C–O stretching modes in the neutral nickel tetracarbonyl complex with different associated frequencies, it is inappropriate to compare any one of these frequencies to the more localized C–O stretching in the C 1s → π^* transition. However, since the C–O stretching frequencies of different symmetries do not differ widely in $Ni(CO)_4$, a mean value of ν_{CO}, obtained by averaging the frequencies, weighted according to the degeneracy of each normal mode, yields a characteristic frequency, $\bar{\nu}_{CO}$, which is approximately independent of the vibrational interaction force constants. This average value is 2075 cm^{-1},[7] which will be used in the following discussion.

There is a substantial reduction of ~170 cm^{-1} in vibrational frequency between ground-state $Ni(CO)_4$ and the C 1s → π^* excited state, similar to the reduction of ~160 cm^{-1} observed for the corresponding processes in CO.[39,41,42] A reduction in frequency is expected due to the promotion of an electron into the C–O π^* antibonding orbitals.

Compared directly with CO gas, the stretching frequency of the excited vibration in the C 1s → π^* transition for the metal complex is slightly lower (1900 vs 1980 cm^{-1}). This result is entirely expected since Ni 3d → π^* back bonding should reduce the C–O bond order. The fact that this reduction in frequency (~80 cm^{-1}) is similar to the difference between the C–O stretching frequency in ground-state CO and the averaged C–O stretching mode of ground-state $Ni(CO)_4$ (~70 cm^{-1}) suggests that a study of the vibrationally resolved core excitation spectra should also provide a reasonable assessment of the metal–ligand bonding situation in metal carbonyl complexes. This observation also supports the view that for the 1s → π^* excitation in $Ni(CO)_4$ the final orbital is effectively localized on the CO group containing the core hole.

We can also compare the vibrational frequency observed in this work with the averaged vibrational frequencies ($\bar{\nu}_{CO}$) of the isoelectronic transition-metal carbonyl complexes $[Co(CO)_4]^-$ (1910 cm^{-1})[76,77] and $[Fe(CO)_4]^{2-}$ (1790 cm^{-1}).[76,77] It can be seen that the C 1s → π^* excited $Ni(CO)_4$ containing a C 1s hole has a C–O frequency (1900 cm^{-1}) approximately the same as that for the $[Co(CO)_4]^-$ ion (1910 cm^{-1}). The lower value for $[Co(CO)_4]^-$ compared to ground-state $Ni(CO)_4$ (2075 cm^{-1}) arises due to more diffuse Co 3d orbitals, hence greater back bonding and higher π^* electron density. The extra π^* electron density in C 1s excited $Ni(CO)_4$ compared with ground-state $Ni(CO)_4$ is therefore similar to the additional π^* electron density due to back bonding in the $[Co(CO)_4]^-$ ion but less than in the dianion $[Fe(CO)_4]^{2-}$.

The final feature of the C 1s high-resolution spectra worthy of note is that the vibrational components of the $Ni(CO)_4$ spectrum are substantially broader than those of the CO spectrum. Since the instrumental resolution was equivalent for collection of these two spectra, the bands of the metal complex must be intrinsically wider. One explanation is that the excited states have shorter lifetimes, and hence their energies are less well defined. However, this effect should give rise to purely Lorentzian broadening of the peaks, whereas the curve fits reveal that their shape is more Gaussian-like in $Ni(CO)_4$ (Gaussian/Lorentzian area ratio 0.889 in $Ni(CO)_4$ vs 0.691 in CO). A more likely explanation is therefore that there is simultaneous excitation of additional vibrational modes in $Ni(CO)_4$, possibly the Ni–C modes, which have very low vibrational frequencies (~400 cm^{-1}).

Interpretation of the remainder of the features in the inner-shell spectra is less straightforward. The 1s → *delocalized* π^* transitions are expected (see above discussion) at ~2.2 eV higher excitation energy than the 1s → *localized* π^* bands, so that either or both of the peaks (numbers 2 and 3, Table I, Figure 2) in the C 1s spectrum with term values of 4.44 and 3.57 eV (or weak underlying features) could be assigned to these transitions. However, excitations to the $9a_1$ (Ni 4s) and $11t_2$ (Ni 4p) orbitals should also occur in this energy range, plus orbitals derived from the CO $3s\sigma$ Rydberg orbitals (by analogy with the term values for the corresponding transitions in CO[39,41]). Indeed, that the O 1s spectrum does not contain a peak with a term value of 4.44 eV argues for its assignment in the C 1s spectrum to orbitals containing no or very little O 2s or 2p character. The preferred assignment is therefore to $11t_2$ (Ni 4p) and/or $9a_1$ (Ni 4s) at a term value of 4.44 in the C 1s spectrum and delocalized π^* plus orbitals of mainly CO $3s\sigma$ character at a term value of ~3.6 eV (C 1s and O 1s spectra). Likewise the lack of a band at a term value of ~2 eV in the O spectrum suggests final orbitals with little O character for the peak (number 4) at $T = 2.07$ eV in the C 1s spectrum. Therefore the most reasonable assignments for this band would be to Ni 5s and/or 5p Rydberg orbitals. The remaining preedge features in both spectra must be assigned in a general fashion to transitions to Rydberg orbitals. The extremely large number of orbitals involved and the lack of any sharp

(56) Bagus, P. S.; Schaefer, H. F. *J. Chem. Phys.* **1972**, *56*, 224.
(57) Cooper, G.; Sze, K. H.; Brion, C. E. High resolution ISEELS and VSEELS Spectra of $Cr(CO)_6$, $Mo(CO)_6$ and $W(CO)_6$. Manuscript in preparation.

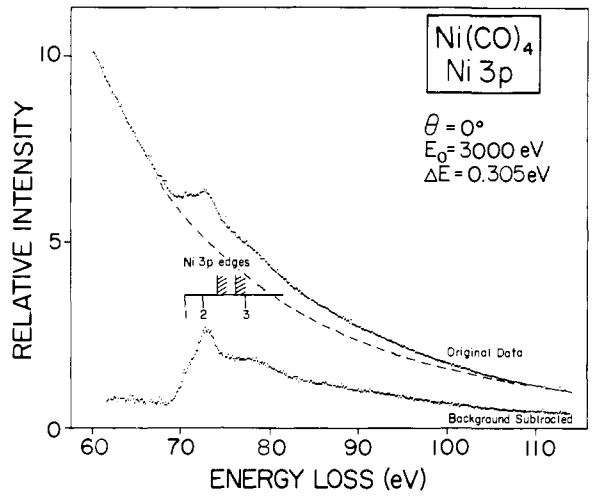

Figure 5. Nickel 3p electron energy loss spectrum of $Ni(CO)_4$.

structure in the spectra at smaller term values prevents any further analysis.

The C 1s and O 1s spectra of $Ni(CO)_4$ show features similar to the corresponding spectra of free CO above their respective ionization edges. By analogy the very broad features at term values of −10.65 eV (C 1s) and −9.96 eV (O 1s) may be assigned to localized σ^* molecular shape resonances (see the above discussion) in the l = 3 (f-like) ionization channels. Such continuum shape resonances have been observed previously in a number of small molecules,[47,58-63] including free CO.[39,44] Recently it has been proposed that there is some correlation between the energy of a shape resonance maximum above the ionization threshold and bond length.[59-62] However, the relative magnitudes of the σ^* term values in $Ni(CO)_4$ and CO (Tables I and II) are not consistent with the longer C–O bond in $Ni(CO)_4$.[64] There are at least two possible reasons for this discrepancy:

(a) The much greater orbital relaxation accompanying ionization of the transition-metal complex results in lower ionization energies and hence larger (more negative) term values for the 1s $\rightarrow \sigma^*$ resonances, even though the absolute σ^* virtual orbital energies may be lower due to increased C–O bond lengths.

(b) The different symmetries of CO and $Ni(CO)_4$ result in different symmetries for the σ^* orbitals in the two molecules and thereby quite possibly different energies. Note also that the 1s $\rightarrow \sigma^*$ peak in $Ni(CO)_4$ may be split by symmetry into two bands, although no splitting is evident in the spectra.

The C and O 1s spectra of $Ni(CO)_4$ also exhibit additional features in the continuum at term values ~−2.5 and ~−6 eV. The X-ray photoelectron spectra of a number of first-row transition-metal carbonyls[5] show shake-up bands at ~2 and ~5–6 eV above the main core level photoelectron bands. These have been attributed to metal 3d $\rightarrow$ localized CO π^* excitations[52] (triplet coupled at ~2 eV and singlet coupled at ~5–6 eV) or[17] a combination of metal 3d $\rightarrow$ CO π^* (~2 eV) and ligand-localized CO $\pi \rightarrow \pi^*$ transitions (5–6 eV). These small features may therefore be associated with these shake-up processes. Alternatively, these peaks are sufficiently wide that they may be additional σ^* molecular shape resonances that have no counterpart in the CO 1s spectra. Possibly they are associated with the Ni–C bonds and may be described as Ni–C σ^* shape resonances. The fact that these transitions are weaker in the O 1s spectrum than the C 1s spectrum is consistent with this assignment. Recent NEXAFS results on CO on metal surfaces also suggest the possibility of metal–molecule levels in the near continuum.[65] Note in Figure 2 the great differences between the C 1s spectra of $Ni(CO)_4$ and CO in this spectral region—the intense peak in the CO spectrum at $T = -4.7$ eV which is assigned to double-excitation processes[39,66] is absent in the $Ni(CO)_4$ spectrum and is replaced with the broader features present in both the C 1s and O 1s spectra as discussed above. However, it cannot be ruled out that part of the intensity in this region of the C 1s spectrum is due to double-excitation processes, possibly C 1s $\rightarrow \pi^*$ accompanied by $9t_2$ and/or 2e (Ni 3d) $\rightarrow \pi^*$. The intense double-excitation peak at $T = -4.7$ in the C 1s CO spectrum is also lost when CO is chemisorbed on metal surfaces, as shown by recent NEXAFS results.[67,68]

Table III. Experimental Energies, Term Values, and Possible Assignments of Features in the Ni 3p Electron Energy Loss Spectrum of $Ni(CO)_4$

feature	energy loss, eV	term value, eV $3p_{3/2}$	term value, eV $3p_{1/2}$	possible assignt
1	70.94 (12)	3.3		$3p_{3/2} \rightarrow$ Ni 4s ($9a_1$)
2	72.85 (12)		3.4	$3p_{1/2} \rightarrow$ Ni 4s ($9a_1$)
Ni $3p_{3/2}$ edge	~74.2[a]			
Ni $3p_{1/2}$ edge	~76.2[a]			
3	78.40 (24)	−4.2	−2.2	3p $\rightarrow$ ed max; double excitation; or σ^*(Ni–C) shape resonance

[a] Estimated from the following data:

species	$2p_{3/2}$	$3p_{3/2}$	$3p_{1/2}$	ref
$Ni(CO)_4$	861.1			3, 4
$Ni(CH_3COCHCOCH_3)_2$	860.5		73.5	70
Ni(g)	860.0	73.0	75.0	69

Nickel 3p Spectrum. The energy loss spectrum of $Ni(CO)_4$ near the Ni 3p ionization edge is shown in Figure 5. The upper portion of the figure shows the original experimental data, below this is the same data after subtraction of the estimated contribution of the underlying valence shell continuum. The valence contribution was estimated by fitting a curve of the form AE^{-B} (A and B are constants, E = energy loss) to the experimental data below ~69 eV and extrapolating it to higher energy.

The energies, term values, and proposed assignments of the numbered features in the Ni 3p spectrum are given in Table III. An estimate of the Ni $3p_{3/2}$ ionization energy of nickel tetracarbonyl was made by considering the constant energy difference between the $2p_{3/2}$ and $3p_{3/2}$ core ionization energies for the free Ni atom[69] and also for $Ni(CH_3COCHCOCH_3)_2$[70] (see Table III). Using the same Ni $2p_{3/2}$–$3p_{3/2}$ difference for $Ni(CO)_4$ together with the available $2p_{3/2}$ ionization energy data for $Ni(CO)_4$ provides an estimate of 74.2 eV for the Ni $3p_{3/2}$ ionization energy of $Ni(CO)_4$. The $3p_{3/2,1/2}$ spin–orbit splitting of ~2.0 eV observed for the free Ni atom[69] is also applied to $Ni(CO)_4$.

Although the Ni 3p transitions are of quite low intensity and are superimposed on the intense underlying valence-shell continuum, at least three features can be distinguished (see Figure 5). The term values of the two peaks below the (estimated) Ni 3p ionization edge are rather low for their assignment to 3p $\rightarrow \pi^*$ transitions. Although term values of transitions to the same final virtual valence orbitals are generally expected to decrease in going from core excitation to valence excitation,[71] the term values for peaks 1 and 2 in the Ni 3p spectrum are lower than

(58) Piancastelli, M. N.; Lindle, D. W.; Ferret, T. A.; Shirley, D. A. *J. Chem. Phys.* **1987**, *86*, 2765.
(59) Stohr, J.; Gland, J. L.; Eberhardt, W.; Outka, D.; Madix, R. J.; Sette, F.; Koestner, R. J.; Doebler, U. *Phys. Rev. Lett.* **1983**, *51*, 2414.
(60) Hitchcock, A. P.; Beaulieu, S.; Steel, T.; Stohr, J.; Sette, F. *J. Chem. Phys.* **1984**, *80*, 3927.
(61) Stohr, J.; Sette, F.; Johnson, A. L. *Phys. Rev. Lett.* **1984**, *53*, 1684.
(62) Sette, F.; Stohr, J.; Hitchcock, A. P. *J. Chem. Phys.* **1984**, *81*, 4906.
(63) Hitchcock, A. P.; Brion, C. E. *J. Phys. B* **1981**, *14*, 4399.
(64) Gumhalter, B.; Wadelt, K.; Avouris, Ph. *Phys. Rev. B* **1988**, *37*, 8048.
(65) Somers, J.; Kordesch, M. E.; Lindner, Th.; Conrad, H.; Bradshaw, A. M.; Williams, G. P. *Surf. Sci.* **1987**, *188*, L693.
(66) Shaw, D. A.; King, G. C.; Cvejanovic, D.; Read, F. H. *J. Phys. B* **1984**, *17*, 2091.
(67) Stohr, J. *X-Ray Absorption: Principles, Applications, Techniques of EXAFS, SEXAFS and XANES*; Wiley: New York, 1987.
(68) Stohr, J.; Sette, F.; Johnson, A. L. *Phys. Rev. Lett.* **1984**, *53*, 1684.
(69) Lotz, W. *J. Opt. Soc. Am.* **1970**, *60*, 206.
(70) Perera, J. S.; Frost, D. C.; McDowell, C. A. *J. Chem. Phys.* **1980**, *72*, 5151.
(71) Robin, M. B. *Higher Excited States of Polyatomic Molecules*; Academic Press: New York, 1985; Vol. III.

Table IV. Experimental Energies, Term Values, and Possible Assignments of Features in the Valence-Shell Electronic Spectrum of $Ni(CO)_4$

	$Ni(CO)_4$					
feature	energy loss, eV	term value ($9t_2$), eV	term value (2e), eV	term value ($5\sigma + 1\pi$), eV	term value (4σ), eV	possible assgnt
1	4.49 (12)	4.23				$9t_2(3d) \rightarrow$ Ni 4s, $10t_2(\pi^*)$
2	5.36 (12)	3.30	4.25			$9t_2(3d) \rightarrow 10t_2(\pi^*)$
3	5.97 (12)	2.75	3.70			$9t_2(3d) \rightarrow 2t_1(\pi^*)$; $2e(3d) \rightarrow$ Ni 4s, π^*
4	6.71 (12)		2.93			$2e \rightarrow$ Ni $2e(3d)$ π^*
$9t_2$ edge	8.72[a]					
2e edge	9.67[a]					
5	10.1 (2)			4.0		
6	12.5 (2)			1.6		CO $(5\sigma + 1\pi) \rightarrow \pi^*$
7	13.7 (2)			0.4	4.6	
$5\sigma + 1\pi$ edge	14.10[a]					
8	14.7 (2)				3.6	
9	15.6 (2)				2.7	
10	17.0 (5)					
4σ edge	18.25[a]					
11	18.9 (5)					
12	22.0 (5)					

[a] From ref 1.

those proposed for the valence level $\rightarrow \pi^*$ transitions (see below). Since $3p \rightarrow \pi^*$ excitations are allowed by electric dipole selection rules, it may be that the π^* orbitals are localized too heavily on the ligand atoms for these transitions to be intense enough to be detected. The two observed peaks are therefore assigned to $3p_{3/2} \rightarrow$ Ni 4s (term value 3.34 eV) and $3p_{1/2} \rightarrow$ Ni 4s (term value 3.4 eV). The splitting of these two peaks ($\sim$2 eV) is comparable to the spin–orbit splitting of the 3p hole state in the free Ni atom.[69,72] That the relative intensities of the lower energy and higher energy peaks do not reflect the $3p_{3/2}$:$3p_{1/2}$ spin–orbit degeneracies may be caused by exchange interactions in the excited state being of comparable magnitude to the spin–orbit interaction.[73]

The broad feature $\sim$4.5 eV above the estimated 3p ionization threshold may be the consequence of a cross-section maximum in the $p \rightarrow \epsilon d$ ionization channels. Such maxima are well-known from atomic cross-section studies by photoabsorption and photoelectron spectroscopy.[74] Alternatively this feature may result from double-excitation processes.

Valence-Shell Spectrum. Figure 6 shows the high-resolution valence-shell electron energy loss spectrum of $Ni(CO)_4$, together with a spectrum of CO obtained at the same resolution (0.068 eV fwhm). The insert shows a least-squares fit of four Gaussian curves to the first band system in the $Ni(CO)_4$ data. Spectra obtained at higher resolution (0.036 eV fwhm) revealed no additional structure. It is apparent from Figure 6 that the percentage of CO gas in the sample of the metal complex is very low and that all the identified features are due solely to $Ni(CO)_4$. The energies, term values, and proposed assignments of the numbered features in the $Ni(CO)_4$ spectrum are presented in Table IV.

The electronic photoabsorption spectrum of gaseous nickel tetracarbonyl has been previously reported over the energy range 4–6.5 eV.[7] The present data show almost quantitative agreement with ref 7, except that a careful deconvolution procedure yields a lower estimate of the energy (by $\sim$0.7 eV) for the first band (see Figure 6b). Gray[6] has reported a spectrum of $Ni(CO)_4$ in a solid CO matrix.

Above the first ionization energy, $\sim$9 eV, detailed assignments are complicated by overlap of the continuum oscillator strength with discrete transitions and the lack of sharp structure in this spectral region. In addition, no suitable calculations are available so that comparison with theory is also not feasible. However, we

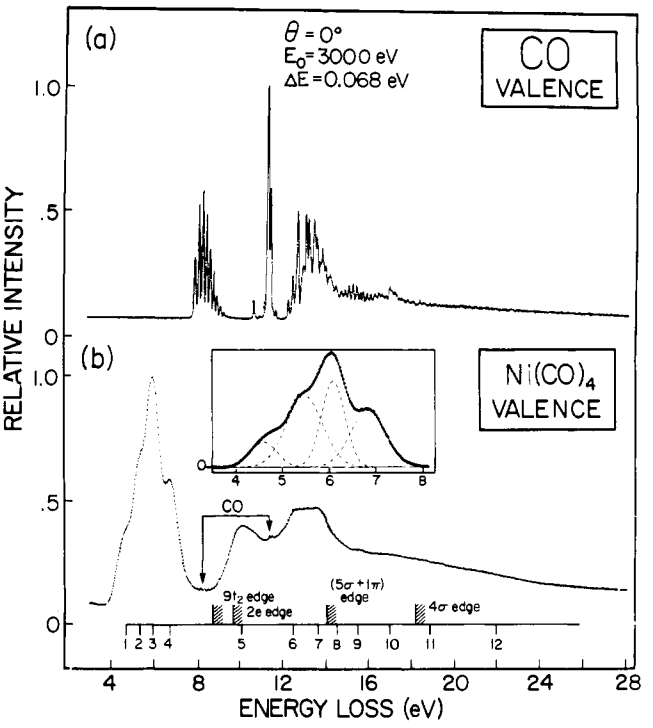

Figure 6. Valence-shell electron energy loss spectrum of $Ni(CO)_4$. The insert shows a fit of four Gaussian curves (see text for details) to the low-energy band system from 4 to 8 eV.

propose the following tentative assignments on the basis of the photoelectron spectrum of $Ni(CO)_4$[1,2] and calculated molecular orbital energy levels:[2,7,16-19,22]

(1) The broad structure (peak 5) at $\sim$10-eV energy loss is due to transitions from the highest energy CO $(5\sigma + 1\pi)$ levels into the π^* orbitals, plus a rise in the Ni 3d ($9t_2$ and 2e) ionization continuum just above threshold.

(2) The "plateau" from $\sim$12.5 to $\sim$13.7 eV energy loss is caused by transitions from the main bulk of CO localized 5σ and 1π levels to the π^* orbitals.

Note that these arguments ignore the possibility of many-electron excitations and are based purely on an independent-particle picture.

We turn now to the low-energy band system from $\sim$4- to 8-eV energy loss. A number of assignments for the region have been suggested previously. In ref 6 the lowest energy band was assigned to the transition $9t_2$ (Ni 3d) $\rightarrow 10t_2$ (π^*), while the most intense peak was assigned in a general fashion to the remainder of the Ni 3d ($9t_2$ + 2e) $\rightarrow \pi^*$ transitions. More detailed assignments have been attempted on the basis of extended Hückel molecular

(72) *Handbook of X-ray and Ultraviolet Photoelectron Spectroscopy*; Briggs, D., Ed., Heyden: London, 1977.
(73) Wendin, G. *Phys. Rev. Lett.* **1983**, *53*, 724.
(74) Manson, S. T. *Adv. Electron. Electron Phys.* **1976**, *41*, 73.
(75) Siegbahn, K.; Nordling, C.; Johansson, G.; Hedman, J.; Hedman, P. F.; Hamrin, K.; Gelius, U.; Bergmark, T.; Werme, L. O.; Manne, R.; Baer, Y. *ESCA Applied to Free Molecules*; North-Holland: Amsterdam, 1969.
(76) Nakamoto, K. *Infra-red Spectra of Inorganic Coordination Compounds*; Wiley: New York, 1963.
(77) Braterman, P. S. *Metal Carbonyl Spectra*; Academic Press: London, 1975; p 190.

orbital calculations[7] and more recently by using configuration interaction on CNDO-type molecular wave functions.[22]

Four components of the 4–8-eV band are resolved in the present work, and the insert to Figure 6 shows that the spectrum fits well to four Gaussian curves, the parameters of which are as follows: peak 1, position 4.49 eV, fwhm 0.667 eV, relative area 0.261; peak 2, position 5.36 eV, fwhm 0.909 eV, relative area 1.0; peak 3, position 5.97 eV, fwhm 0.582 eV, relative area 0.774; peak 4, position 6.71 eV, fwhm 0.881 eV, relative area 0.766. It is obvious from the figure that peaks 1 and 3 and 2 and 4 have similar widths, suggesting that these pairs may have a common initial state. Since transitions from the triply degenerate $9t_2$ set of Ni 3d orbitals are expected at lower energies than peaks due to promotion of electrons from the doubly degenerate 2e set, this would lead to the conclusion that peaks 1 and 3 originate from the $9t_2$ MOs and peaks 2 and 4 from the 2e MOs. However, even though the transition matrix elements will certainly be quite different for the $9t_2$ and 2e orbitals, it is unlikely that they are so different as to result in the experimental $(1 + 3)/(2 + 4)$ intensity ratio of 0.586, considering the 3:2 ($9t_2$:2e) degeneracy ratio and the fact that more of the low-energy transitions involving the 2e orbitals are symmetry forbidden. More likely the observed band widths are the result of heavily overlapping transitions and/or associated vibrational progressions.

The assignment given in ref 7 involved transitions from the CO localized $(5\sigma + 1\pi)$ levels giving rise to a number of components of the low-energy band system (i.e., the bands below ~8 eV). However, relative to the $(5\sigma + 1\pi)$ ionization onset, the highest energy loss (lowest term value) component of this band system (peak 4) at ~6.7-eV energy loss would then have a term value of ~7.4 eV, which is higher than the term value for any band in the inner-shell spectra (see Tables I–III). Since term values for a particular final virtual valence orbital tend to decrease in going from core excitation to valence excitation,[71] such an assignment can be eliminated on these grounds.

The configuration interaction calculations[22] came to the conclusion that not only is the manifold of π^* orbitals accessible from ~4 to 6 eV but so also are the Ni 4s and 4p orbitals, although many of the possible transitions were calculated to be weak. Their assignment of the most intense peak at ~6 eV was to metal → ligand charge transfer, $9t_2$ (Ni 3d) → $2t_1$ (π^*), the first lower energy shoulder at ~5.5 eV to $9t_2$ (Ni 3d) → $10t_2$ (π^*), and the lowest energy band to either $9t_2$ (Ni 3d) → Ni 4s or $10t_2$ (π^*) triplet coupled. If the lowest energy transition is indeed the latter, then it must gain intensity through vibronic coupling, since exchange transitions are forbidden at the high impact energies and 0° scattering angle used in the present VSEELS work. Unfortunately these calculations[22] did not consider transitions involving the 2e (Ni 3d) electrons. Assuming the above assignment[22] to be correct, the excitations from the lower lying 2e (Ni 3d) orbitals can then be assigned either wholly to the peak centered at ~6.7-eV energy loss (feature 4) or partly to this peak plus some intensity contributing to the 5.97 eV peak (feature 3). These findings of the CI calculations[22] are reflected in the assignments summarized in Table IV. It is hoped that the results reported here will stimulate further theoretical investigations of the valence-shell photoabsorption spectrum of $Ni(CO)_4$ to clarify this situation.

Conclusions

We have obtained the first ISEELS spectra of a gaseous transition-metal complex, $Ni(CO)_4$. The VSEELS spectrum was also obtained over an extended energy range. The inner-shell spectra could be interpreted largely by analogy with those of free CO. In particular the C 1s and O 1s spectra both show intense 1s → π^* and 1s → σ^* transitions for $Ni(CO)_4$ and free CO. Vibrational structure associated with a C–O stretching mode was resolved in the 1s → π^* bands of the C 1s spectra. The $Ni(CO)_4$ inner-shell spectra can most readily be explained by invoking localization of the C 1s or O 1s hole on one of the CO groups. The shifts in 1s → π^* transition energies and term values from free CO were interpreted in terms of severe orbital relaxation upon creation of a 1s hole and also the influence of Ni → CO π back bonding. The changes in vibrational structure between $Ni(CO)_4$ and CO in the C 1s → π^* band, in particular a lower C–O vibrational frequency in $Ni(CO)_4$, also show direct evidence for metal–ligand back bonding.

Due to the complicating factor of greater orbital relaxation accompanying creation of a 1s hole in $Ni(CO)_4$, quantitative estimates of the extent of back bonding are not possible. However, the ISEELS technique should be very valuable in the investigation of metal–ligand bonding when results for different metal carbonyls can be compared, since then the extent of orbital relaxation should be almost constant for a given series of compounds. We are presently undertaking a study of the group VIA metal hexacarbonyls to investigate further the applicability of ISEELS spectroscopy to studies of transition metal–ligand bonding.

Acknowledgment. Financial support for this work was provided by NSERC (Canada). A University of British Columbia Graduate Fellowship (K.H.S.) and an SERC (UK)/NATO Postdoctoral Fellowship (G.C.) are acknowledged. We are indebted to Dr. A. P. Hitchcock for his many helpful comments and suggestions concerning this work.

Registry No. CO, 630-08-0; $Ni(CO)_4$, 13463-39-3.

Experimental Electronic Structures of Complexes of SO_2: An Electron Spectroscopic Study

T. Pradeep, C. S. Sreekanth, M. S. Hegde, and C. N. R. Rao*

Contribution No. 580 from the Solid State and Structural Chemistry Unit, Indian Institute of Science, Bangalore 560 012, India. *Received November 21, 1988*

Abstract: He I photoelectron spectra of gas-phase complexes formed by SO_2 with the electron donors trimethylamine, triethylamine, diethyl ether, and diethyl sulfide have been recorded and bands assigned to the different orbitals based on MO calculations. The shift in the ionization energy of the lone pair orbital of the donor in these complexes is shown to vary proportionally with the dissociation energy as well as the magnitude of charge transfer to SO_2. Electron energy loss spectra of the donor–SO_2 complexes have been recorded to characterize the electronic transitions in the vacuum UV region. Only the amine–SO_2 complex shows a band ascribable to a charge-transfer transition. In order to investigate situations where SO_2 acts as an electron donor, He I spectra of complexes with BF_3 and HCl have been measured. The decrease in the Mulliken population of SO_2 as well as the dissociation energy of these complexes varies parallel to the shift in the lone pair ionization energy of SO_2.

The 1:1 charge-transfer complex between trimethylamine and sulfur dioxide has been characterized adequately both in the gas and the condensed phases.[1-3] The gas-phase dissociation energy of the complex[3] is 40.5 kJ mol^{-1}. The complex has essentially a

0002-7863/89/1511-5058$01.50/0